

## Stress Wave Scattering: Friend or Enemy of Non Destructive Testing of Concrete?\*

Dimitrios G. AGGELIS\*\*, Tomoki SHIOTANI\*\*\*, Theodore P. PHILIPPIDIS\*\*\*\*  
and Demosthenes POLYZOS\*\*\*\*

\*\*Research Institute of Technology, Tobishima Corporation, 5472 Kimagase, Noda-shi,  
Chiba 270-0222, Japan

E-mail: dimitris-tobishima@t-msweb.net

\*\*\*Department of Urban Management, Graduate School of Engineering Kyoto University C1-2-236,  
Kyoto-Daigaku-Katsura, Nishikyo-Ku Kyoto 615-8540, Japan,

\*\*\*\*Department of Mechanical Engineering and Aeronautics, University of Patras, Rion 26504, Greece,

### Abstract

Cementitious materials are by definition inhomogeneous containing cement paste, sand, aggregates as well as air voids. Wave propagation in such a material is characterized by scattering phenomena. Damage in the form of micro or macro cracks certainly enhances scattering influence. Its most obvious manifestation is the velocity variation with frequency and excessive attenuation. The influence becomes stronger with increased mis-match of elastic properties of constituent materials and higher crack content. Therefore, in many cases of large concrete structures, field application of stress waves is hindered since attenuation makes the acquisition of reliable signals troublesome. However, measured wave parameters, combined with investigation with scattering theory can reveal much about the internal condition and supply information that cannot be obtained in any other way. The size and properties of the scatterers leave their signature on the dispersion and attenuation curves making thus the characterization more accurate in case of damage assessment, repair evaluation as well as composition inspection. In this paper, three indicative cases of scattering influence are presented. Namely, the interaction of actual distributed damage, as well as the repair material injected in an old concrete structure with the wave parameters. Other cases are the influence of light plastic inclusions in hardened mortar and the influence of sand and water content in the examination of fresh concrete. In all the above cases, scattering seems to complicate the propagation behavior but also offers the way for a more accurate characterization of the quality of the material.

**Key words:** Attenuation, Concrete, Damage, Dispersion, Frequency, Mortar, Scattering, Velocity

### 1. Introduction

Stress wave propagation is used for many decades for non destructive inspection of concrete. The most widely used feature is the pulse velocity which has been correlated with strength and damage since long ago<sup>(1)-(3)</sup>. Attenuation related features seem to be even more indicative of the internal condition<sup>(4)(5)</sup>. In any inhomogeneous material as concrete a dominant wave propagation mechanism is scattering<sup>(6)-(8)</sup>. When a propagating wave encounters obstacles, this leads to velocity variation with frequency and high attenuation.

These obstacles could be voids, cracks or other inclusions with properties different from the matrix material. Scattering, combined with damping of concrete materials results in low amplitude of stress waves and therefore in many cases hinders the examination in situ. This is especially true for large and damaged components. However, study of their dispersive and attenuative behavior can enhance the characterization due to interaction with the inhomogeneity parameters.

## 2. Stress wave scattering

When a propagating wave impinges on a spherical elastic object a part of energy is refracted into the scatterer and another is scattered over many directions. In order to determine the energy pattern after each impact, the continuity of stresses and displacements on the surface of the scatterer can be used <sup>(9)</sup>. In order to generalize the result for an assembly of scatterers, dispersion relations have been proposed <sup>(10)(11)</sup>. These relations combine the wavenumber of the matrix material,  $k_c$  with the complex wavenumber of the composite material,  $k$  and hence the frequency dependent velocity and attenuation can be calculated. A widely used relation is <sup>(11)</sup>:

$$\left(\frac{k}{k_c}\right)^2 = 1 + \frac{3\varphi}{k_c^2 R^3} f(0) + \frac{9\varphi^2}{4k_c^4 R^6} [f^2(0) - f^2(\pi)] \quad (1)$$

where  $R$  is the scatterer radius,  $\varphi$  is the particle volume concentration, and  $f(0)$  and  $f(\pi)$  are the forward and backward far-field scattering amplitudes respectively, showing what part of energy is scattered forward and backward.

The frequency dependent phase velocity  $C(\omega)$  and attenuation  $\alpha(\omega)$  are calculated from the complex wavenumber of the medium:

$$k(\omega) = \frac{\omega}{C(\omega)} + i\alpha(\omega) \quad (2)$$

where  $\omega$  stands for radial frequency.

It is understood that the mechanical properties of the constituent materials, scatterer size and volume content, as well as the propagating wavelength are all important in this case.

The goal of such an approach is to calculate the wavenumber of a homogeneous dispersive material, equivalent to the actual material that consists of the matrix and the inclusions. An example of such a model for concrete can be seen in Fig. 1. The spherical shape is generally used for simplicity and is considered a good approximation due to random orientation of actual inclusions. It is mentioned that although the constituent materials can be perfectly elastic and non dispersive, the propagation in a composite medium is generally dispersive.

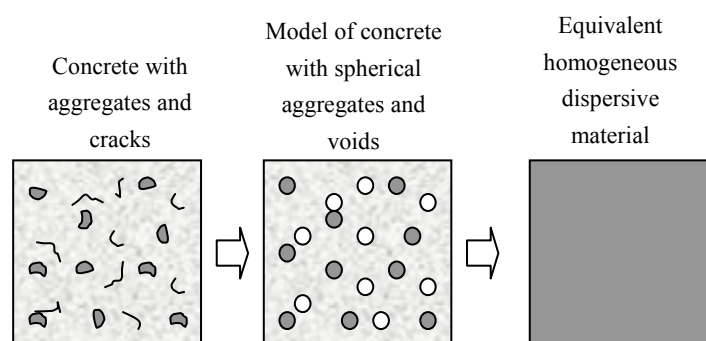


Fig. 1. Concrete model used in scattering investigation.

In many cases scattering results in behaviors not expected according to common knowledge. For example stiff inclusions in a softer matrix do not always increase the measured velocity at certain frequencies <sup>(7)(12)(13)</sup>, or liquids exhibit extraordinarily high velocities with the presence of gas bubbles inside <sup>(14)</sup>. Scattering theory has been proven to predict the wave propagation behavior of inhomogeneous media quite accurately. Following are three cases of stress wave examination of cementitious materials, where scattering mechanisms seem to have strong influence.

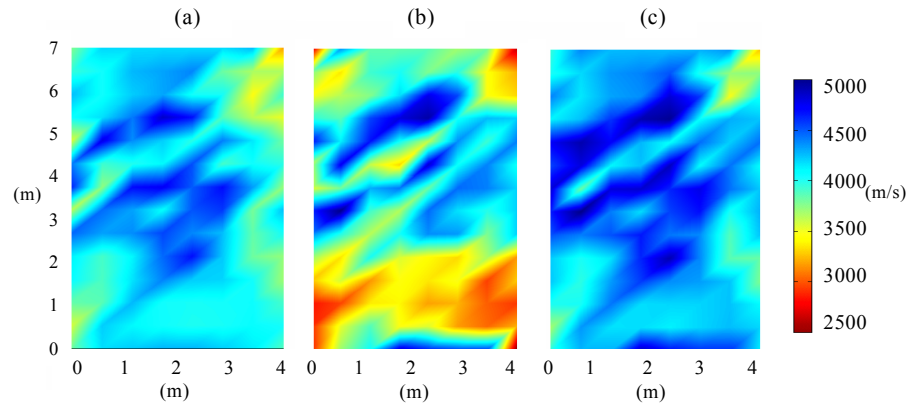


Fig. 2. Tomogram of a dam pier section examined (a) before, (b) after repair, (c) after complete hardening of grout.

### 3. Wave propagation in concrete repaired with cement injection

The present case concerns an old moderately deteriorated concrete dam. In order to reinforce the piers and decrease the permeability, cementitious grout was injected. This was conducted by drilled boreholes and it was assumed to fill a substantial part of the interconnected network of cracks. Stress wave tomography at several sections of the piers was conducted before and after repair while details about the whole monitoring project and the tomography software used can be found in <sup>(15)(16)</sup>. In Fig. 2(a) the tomogram of a cross section before injection of grout is depicted. The general condition can be characterized satisfactory since the propagation velocity is generally higher than 3500 m/s, except some small areas. However, two weeks after repair, the tomogram showed clearly decreased velocity, even as low as 2500 m/s, see Fig. 2(b). This behavior was not expected since cementitious material replaced the voids.

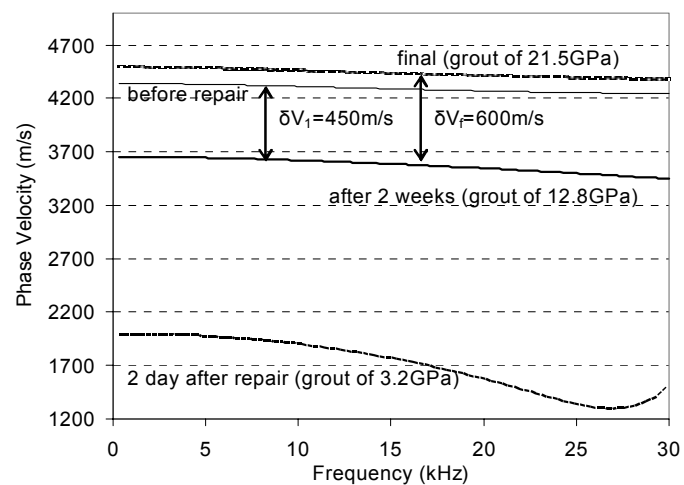


Fig. 3. Theoretical dispersion curves for concrete at different ages of grout and 15% voids.

Even if the defects were not completely eliminated, the velocity is not supposed to decrease. The reason as revealed after application of scattering theory was the interaction of the waves with the grout material that acted as a pattern of distributed scatterers into the concrete matrix. This behavior was highlighted due to low temperatures at that part of the year that delayed considerably the hardening of grout, resulting in high acoustic impedance mis-match between the inclusions and the matrix.

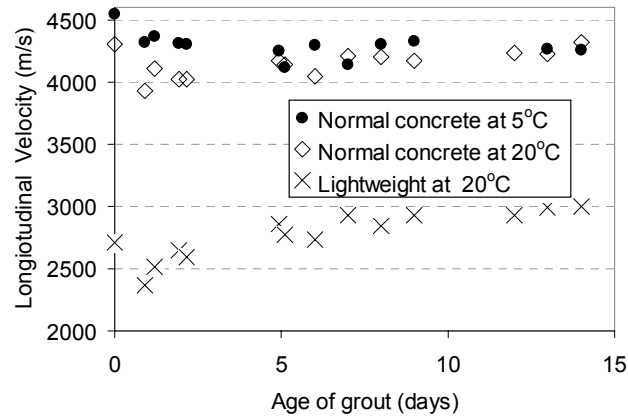


Fig. 4. Longitudinal velocity of porous concrete specimens impregnated with grout vs. age of grout.

Application of scattering theory yielded theoretical results concerning i) the damaged state, assuming scattering on cavities embedded in the concrete matrix, ii) the freshly repaired structure where the cavities were replaced by soft elastic scatterers and iii) the same matrix after complete hardening of the grout scatterers. The mechanical properties of concrete applied to the model were measured from retrieved cores from the dam. As to the grout material properties, ultrasonic experiments were conducted in specimens of grout casted in laboratory. Therefore, longitudinal and Rayleigh wave velocities were measured at different ages<sup>(17)</sup> and the modulus of elasticity  $E$  and the Poisson's ratio,  $\nu$  were calculated. In the present case the age of two weeks was of interest since at that time the post monitoring with stress waves took place, as well as the age of one year until which it was assumed that the hydration was completed. In Fig. 3 one can see theoretical predictions using scattering theory for the problem at hand for the low frequency band 0-30 kHz<sup>(17)</sup>. The velocity of material with 15% cavities (before repair) is around 4300 m/s. When in stead of cavities, 15% scatterers of 12.8 GPa are applied (corresponding to fresh grout of two weeks) it is seen that the velocity for this entire band is decreased by about 450m/s. When scatterers of 21.5 GPa are applied (completely hardened grout) the velocity is elevated even higher than the initial porous state. Therefore, it is obvious that filling the cavities with any material should not be expected to automatically increase the velocity. Indeed if the properties of very fresh grout are applied (i.e. 3.2 GPa, see again Fig. 3), the velocity can be even lower than 2000 m/s.

Using scattering theory one can calculate the velocity at any given frequency. However, only lower band results are presented since the actual experiment at site was limited to frequencies lower than 20 kHz.

As shown earlier in Eq. (1) and Eq. (2), the volume content of the scatterers is strongly connected to the resulting velocity. Therefore, from the velocity decrease at any point of the structure (or tomogram cell) the volume content of grout can be estimated. Then, the scattering problem is solved for each cell assuming this volume to be occupied by completely hydrated grout (i.e.  $E=21.5$  GPa,  $\nu=0.2$ ). This way the final velocity corresponding to each cell (or any specific area of the cross section) is calculated<sup>(17)</sup>. The



result is depicted in Fig. 2(c). The final velocity structure reveals an average increase of 250 m/s, something that was not evident two weeks after grouting due to very low stiffness of grout. This was partially a result of the low temperatures (below 0° C) that considerably delayed the hardening of grout and the eventual increase of velocity.

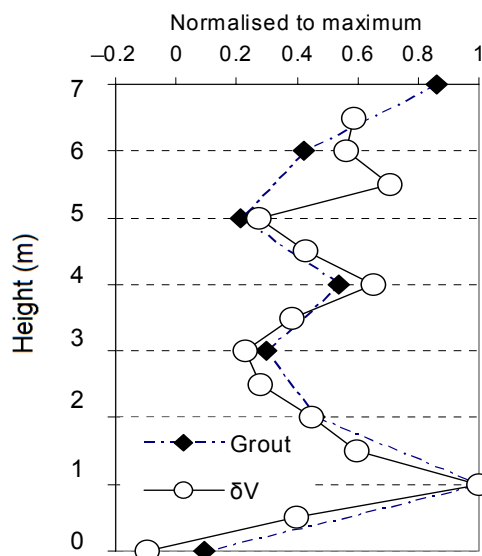


Fig. 5. Amount of grout injected and velocity decrease after application of grout according to the height of structure, (normalized to maximum).

It is mentioned that another approach through static homogenization models can be followed. Such models have been used for the estimation of the effective mechanical properties of particulate composites in general <sup>(18)(19)</sup> or specifically for concrete <sup>(20)</sup>. Applying in any of the above models, the material properties concerning the case before repair ( $E_{matrix}=35$  GPa,  $E_{voids}=0$  GPa) the calculated effective modulus of elasticity is 28.6 GPa. Combined with the density of 2070 kg/m<sup>3</sup>, (calculated for concrete with 15% voids) results in velocity of 3921 m/s. Replacing the voids with two weeks old grout of  $E_{inc}=12.8$  GPa in the same matrix, ( $E_{matrix}=35$  GPa) the effective modulus is calculated to 31.9 GPa. With the new density of 2220 kg/m<sup>3</sup>, the velocity is calculated to 3995 m/s. Therefore, it is seen that a static homogenization approach is not enough to explain the observed behavior, since it predicts a velocity increase, even small, while in the actual case a large decrease was measured.

In order to validate this explanation, ultrasonic measurements were conducted in porous concrete specimens in laboratory environment before and after they were impregnated with grout. The results, as seen in Fig. 4, showed a certain decrease of pulse velocity (around 10%) immediately after impregnation for all three specimens, even though the porous volume had been replaced with cementitious material. Specifically for one specimen that was held in low temperature (5°C) the velocity never recovered, as shown in Fig. 4., highlighting the role temperature plays in wave propagation in grouted structures.

Furthermore, in the actual structure, the amount of grout injected to each borehole was available. It was seen that at the positions where big amount of grout was injected, the velocity decrease was greater, see Fig. 5. For example at the height of 1 m, 241 kg of grout were injected, the maximum quantity of any location. This was accompanied by a severe velocity decrease of more than 800m/s. This shows that the decrease of velocity in such a case should not be interpreted as a sign of unsuccessful repair; on the contrary it shows sufficient filling and is a first step towards the stiffening of the material.

#### 4. Wave propagation in fresh mortar

Another case of strongly scattering medium is the case of fresh cementitious material. The mix proportions (and especially the water to cement ratio) are very important for the future service life of the material. Therefore, examination while it is still in the fresh state is crucial to secure that the material to be placed in the structure is acceptable.

Due to its inhomogeneous nature (liquid cement paste matrix containing sand grains and air bubbles), stress waves are severely attenuated. Although this has been stated <sup>(21)</sup>, the actual mechanism was not absolutely clear.

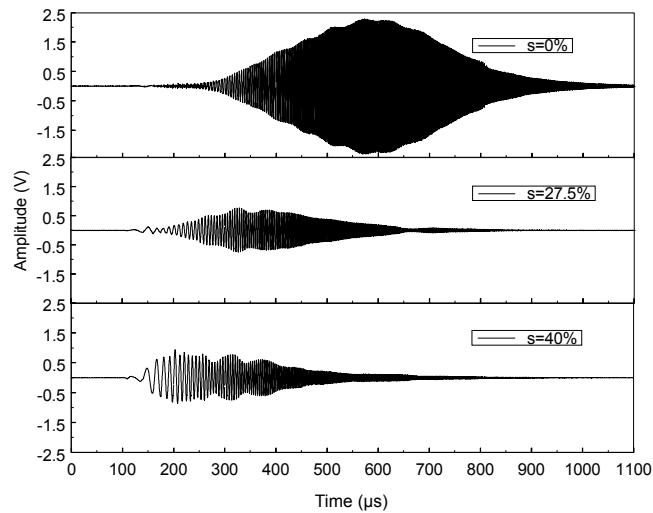


Fig. 6. Time domain sine-sweep pulses from specimens with different sand content.

Mortar with different sand,  $s$ , and water content was tested recently <sup>(22)(23)</sup>. The excitation was a sine-sweep signal, containing frequencies from 10 kHz to 1 MHz with the same magnitude. In Fig. 6 one can see the response of cement paste, mortar with 27.5% of sand and 40%. It is obvious that the increase of sand content diminishes the amplitude, translating simultaneously the energy to the initial part that contains lower frequencies.

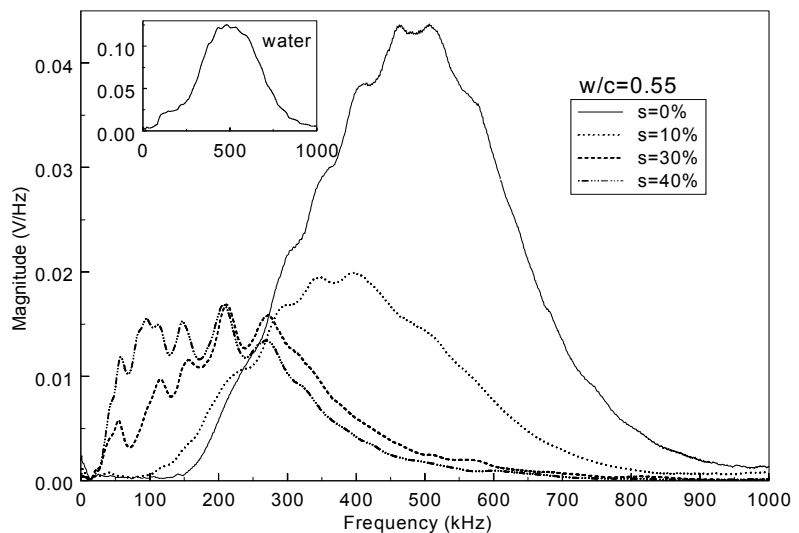


Fig. 7. FFTs of pulses from specimens with different sand content.

In Fig. 7 the Fast Fourier Transform of waveforms collected from different mixtures are depicted <sup>(23)</sup>. It seems that the sand grains act as a cut off filter for higher frequencies, while they facilitate the propagation of lower frequencies.

Since the transmitted pulse is severely dependent on the sand content, this is a certain indication of scattering mechanisms. Scattering theory was used to solve two different problems: I) liquid mortar containing air bubbles and II) liquid matrix containing elastic inclusions (sand grains) <sup>(22)</sup>. In Fig. 8(a) one can see the experimental attenuation of different mixes calculated by the frequency response of each specimen divided by the response of water. In Fig. 8(b) theoretical results of scattering theory are depicted.

It is seen that the measured high frequency attenuation of Fig. 8(a) is followed very closely by the solution of scattering on sand grains, area II. Additionally, the high attenuation of cement paste at low frequencies is explained when considering scattering on the air bubbles, area I.

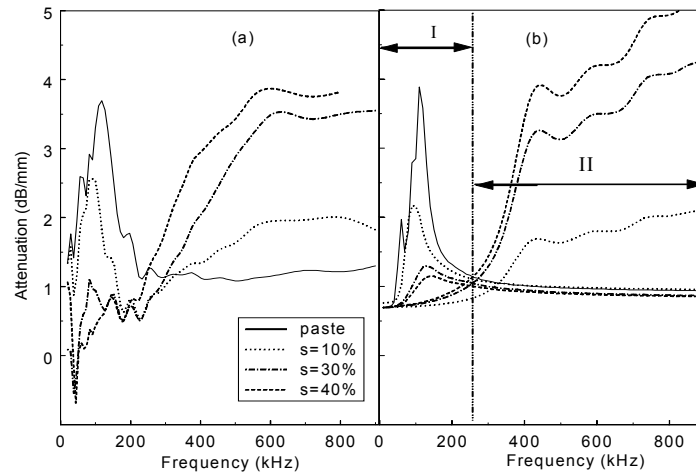


Fig. 8. Comparison of experimental (a) and theoretical (b) attenuation curves of mortar with  $w/c=0.50$ .

Also interesting is the dispersion behavior of fresh mortar. Applying different tone burst signals, the phase velocity of several frequencies was determined <sup>(22)</sup>. In Fig. 9 phase velocities vs. frequencies are depicted for mortar with different sand content. Cement paste containing no sand, exhibited velocities as high as 9000 m/s for a narrow band around 150-175 kHz. This behavior is typical for “bubbly liquids”. Depending on the mean bubble size, there is a narrow band of frequencies where velocities of more than 10000 m/s have been measured for water <sup>(14)</sup>.

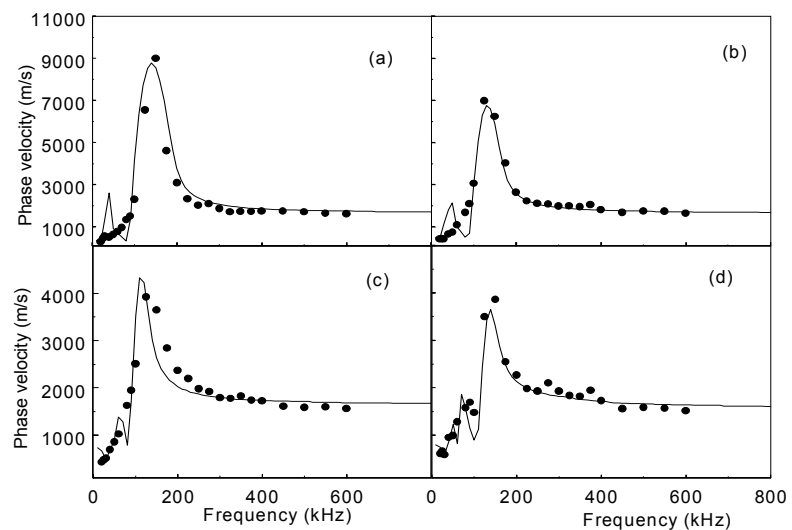


Fig. 9. Phase velocity vs. frequency for mortar with  $w/c=0.55$  and  $s=0\%$  (a), 25% (b), 30% (c) and 40% (d). Dots stand for experimental measurements and solid curves for theoretical predictions.

The experimental behavior is followed very well using scattering theory and assuming a small percentage of 2% of cavities standing for bubbles, as seen by the solid lines of Fig. 9. The different content of sand was simulated by different shear rigidity, since cement paste is very close to a liquid, while sand rich mixes are much stiffer. It seems that the effective shear rigidity of fresh mortar is a key factor for the so called “bubble resonance behavior” and when the shear rigidity is high, this behavior is blocked. The shear modulus is affected by the sand and water content and therefore detailed measurement of phase velocity can help characterize the water to cement ratio. From the whole range of frequencies examined, it is suggested that proper characterization can be achieved focusing on the band of 150-200 kHz, since at this band the composition (water and aggregate content) has a strong influence on velocity, while for higher as well as lower frequencies the behavior of different mixtures do not seem to differ much.

### 5. Dispersion and attenuation due to simulated damage

Another case of strong scattering interaction that is presented in this paper is mortar containing light inclusions, simulating distributed cracks. In order to study the correlation of wave propagation parameters with damage, spherical polystyrene inclusions have been embedded in mortar during casting in other cases <sup>(24)</sup>. The dispersion curve revealed that phase velocity is much influenced especially for lower frequencies. Mortar with 30% volume content of inclusions starts with a phase velocity of 3600 m/s at 200 kHz and rises to 4100 m/s for 1 MHz. This strongly dispersive behavior is attributed to scattering.

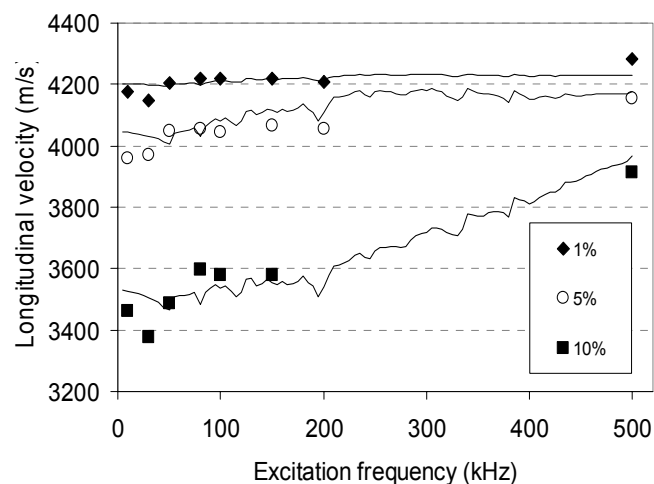


Fig. 10. Pulse velocity vs. frequency for mortar with different “damage” content. Dots stand for experimental measurements and solid curves for theoretical predictions.

In the case presented in this paragraph, the inclusions embedded in mortar are small thin vinyl plates (30x30x0.2 mm), resembling more realistically the actual crack shape. Specimens with different “damage” contents, namely 1%, 5% and 10% were casted. Experimental details can be found in <sup>(25)</sup>. Velocity was measured using narrow band tone bursts with different central frequencies, namely 10, 30, 50, 80, 100, 150 and 500 kHz. Results can be seen in Fig. 10 for any inclusion content (points). It is worth to mention that in any case the material exhibits dispersive behavior. Velocities increase up to the highest frequency tested. Cementitious material is known to exhibit dispersive behavior <sup>(24)(26)-(29)</sup> due to its inhomogeneous nature. The inclusions increase this inhomogeneity and therefore, the velocity variation with frequency. For the case of 10% inclusions the velocity rises from 3400 m/s at 30 kHz to 3900 m/s at 500 kHz, as seen in Fig. 10.



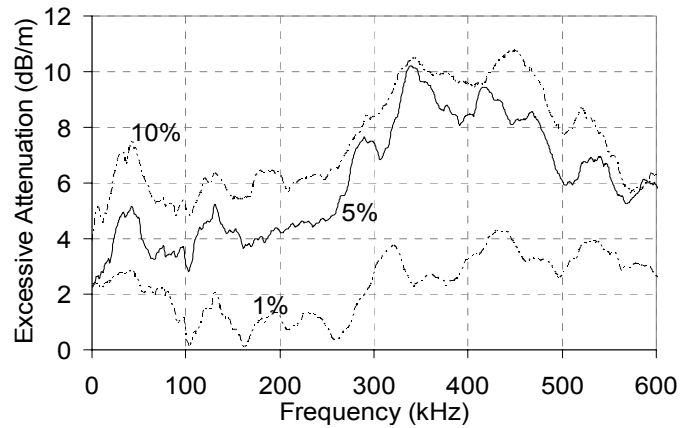


Fig. 11. Frequency dependent excessive attenuation for mortar with different inclusion contents.

Solving the problem of wave propagation in mortar with light inclusions, the trend seems to be explained well. The light inclusions have a dominant effect at lower frequencies as seen by the solid lines of Fig. 10. Since the orientation of the actual particles is random, and in order to follow closer the experimental points, two different populations of spherical inclusions were assumed, one with 3mm radius and another with 15 mm. In practice the workability of the mixes was reduced with increasing plastic content, meaning that an amount of air bubbles were entrapped. Therefore, in the simulation a percentage of air bubbles (cavities) were assumed. The combined effect of soft inclusions and air bubbles seems to explain very closely the experimental behavior throughout the band of 10 kHz-500 kHz.

This dependence of dispersion on inclusion content,  $\phi$ , as seen also in Eq. (1), suggests that measurement at different frequencies can help characterize the material, since sound mortar exhibits only slight dispersion (velocity increase), while heavily damaged (material with a lot of inclusions) exhibits remarkable dispersion. Scattering influences have been studied in different composite materials in the literature. In any case the velocity measured at higher frequencies always converges to the velocity of the matrix, while any discrepancy due to inclusion content is more evident at lower bands<sup>(30),(31)</sup>. This seems to be the case for the present experimental series since for increasing frequency the velocity measured at any specimen becomes closer to that of plain mortar.

As stated earlier, energy related parameters are more sensitive to damage. This is also the case for this experimental investigation. While the pulse velocity is almost the same between sound mortar and material with 1% inclusions, attenuation seems to distinguish between these two cases, as shown in Fig. 11.

Attenuation in this case is calculated from the frequency responses of “damaged” specimens in reference with the response of plain mortar. It is the contribution of the plastic inclusions alone, without considering the attenuation of the mortar itself. Therefore, it is called “excessive attenuation”. Even 1% of damage leads to certain attenuation compared to sound material, while larger discrepancies between sound and damaged are exhibited above 300 kHz. Increasing the inclusion content to 5% and 10%, results in much higher attenuation, as seen in Fig. 11. Although generally stress wave monitoring projects are limited to low frequencies, it is suggested that exploitation of the highest possible frequency component leads to clearer correlations. In order to produce reliable theoretical attenuation curves the numerical simulation of wave propagation in such a material is under way, using the exact geometry of the inclusions. This way it will also be investigated if spherical shape is an adequate approximation of damage or if more realistic shapes should be used.

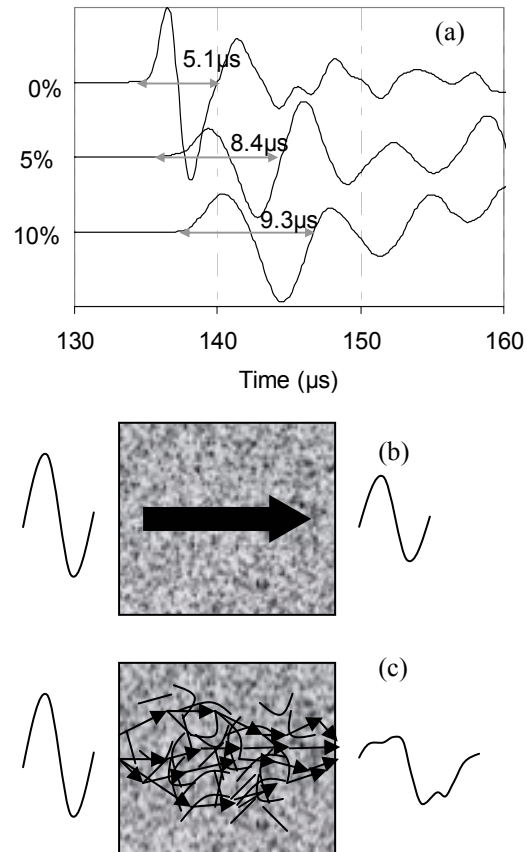


Fig.12. (a) First cycle collected in mortar with different inclusion contents, (b) propagation in homogeneous medium, (c) propagation in strongly scattering medium.

One interesting manifestation of scattering is presented in Fig. 12(a). In this figure, waveforms collected at different materials under the same excitation are depicted. It is clear that as the inclusion content increases, the cycles become broader. This is more likely the effect of the multiple paths traveled by different parts of energy. In a homogeneous material all the energy travels through the shortest (straight) path, see Fig. 12(b). In a strongly scattering medium though, the energy is distributed to many paths with different lengths and transit times, as presented in Fig. 12(c). This results in the broadening of the pulse. The waveform shape distortion with increasing inhomogeneity has been noticed in other cases of strongly scattering media <sup>(13)(28)</sup> and is attributed to the different possible paths the energy can follow in inhomogeneous material.

Finally, another indication and result of scattering is the local variation of propagation characteristics. In Fig. 13(a) it is seen that waveforms collected at different wave paths (of equal length) in a cement paste specimen are identical, with all the peaks synchronized. This is attributed to the homogeneity of the material. In Fig. 13(b) one can see waveforms collected at four different points in mortar. It is seen that the synchronization holds only for the first cycles. Eventually, in Fig. 13(c) it is clear that heavily damaged mortar exhibits different response at any different point. For a given specimen although the overall inclusion content is accurately known, e.g. 10% in this case, changing the position of transducers means that different configuration and orientation of inclusions are encountered by the wavefront. Therefore, the paths that the energy travels through are infinite. This makes any measurement different, and increases the experimental scatter of velocity and attenuation measurements. As a result, care should be taken in order to ensure that the measurements are representative.

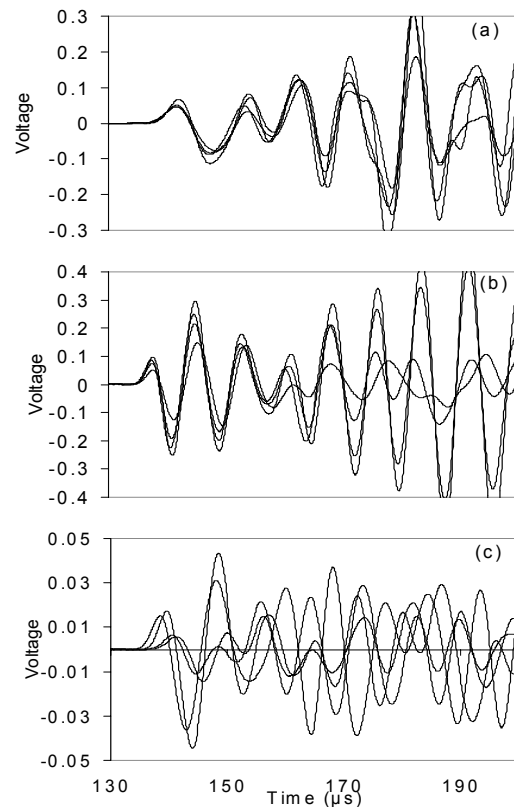


Fig. 13. Waveforms collected at different points in (a) cement paste, (b) mortar and (c) mortar with 10% of inclusions.

## 6. Conclusion

Scattering is a dominant mechanism of wave propagation in inhomogeneous materials. It leads to lower amplitude due to redistribution of energy in different directions making in some cases acquisition difficult. However, the way inhomogeneity interacts with a propagating wave is indicative of its shape and content. Therefore, investigation of wave propagation with scattering theory can lead to reasonable explanations of some phenomena difficult to explain otherwise. Such phenomena are the decrease of the propagation velocity of damaged concrete shortly after repair with cementitious grout, the very high phase velocities of fresh mortar for specific bands of frequencies as well as the highlighted dispersion of mortar containing light inclusions. The experimental behaviors described in this paper are due to strong wave scattering mechanisms. Their study can suggest appropriate ways to characterize the material, e.g. focusing on the indicative wave parameter or using more suitable frequencies. A general remark is that exploitation of energy features is promising as to damage characterization. Attenuation values are more sensitive to coupling effects and therefore more difficult to reliably measure in situ. However, their potential is higher since in laboratory studies, they lead to clearer discrimination between sound and damaged material.

## References

- (1) M. F. Kaplan, *Magazine of Concrete Research*, 11 (32) (1959), pp.85-92.
- (2) S. Popovics, *Materials Evaluation*, 59 (2) (2001), pp.123-130.
- (3) D. A. Anderson, R. K. Seals, *ACI Journal*, 78-9 (1981), pp.116-122.

- (4) S. F. Selleck, E. N. Landis, M. L. Peterson, S. P. Shah, J. D. Achenbach, *ACI Materials Journal*, 95 (1) (1998), pp.27-36.
- (5) S. P. Shah, J. S. Popovics, K. V. Subramanian, C. M. Aldea, *Journal of Engineering Mechanics-ASCE*, 126 (7) (2000), pp.754-760.
- (6) S. V. Tsinopoulos, J. T. Verbis, D. Polyzos, *Advanced Composite Letters*, 9 (3) (2000), pp.193-200.
- (7) L. W. Anson and R. C. Chivers, *Journal of Physics D*, 26 (1993), pp.1566-1575.
- (8) P. Anugonda, J. S. Wiehn, J. A. Turner, *Ultrasonics*, 39 (2001) pp.429-435.
- (9) C.F. Ying, R. Truell, *Journal of Applied Physics*, 27 (9) (1956), pp.1086-1097.
- (10) L. L. Foldy, *Physical Review*, 67 (1945), pp. 107-119.
- (11) P. C. Waterman, R. Truell, *J. Mathematical Physics*, 2 (1961), pp.512-537.
- (12) B. Kaelin and L. R. Johnson, *Journal of Applied Physics*, 84 (1998), pp.5458-5468.
- (13) M. L. Cowan, K. Beaty, J. H. Page, L. Zhengyou, and P. Sheng, *Physical Review E*, 58 (1998), pp.6626-6636.
- (14) S. Temkin, *Journal of the Acoustical Society of America*, 108 (1) (2000), pp.126-146.
- (15) T. Shiotani, D. G. Aggelis, *Structural Faults and Repair-2006*, 13-15 June, Edinburgh, (2006), Paper OCON-SHIO-v2 (in CD-ROM).
- (16) Y. Kobayashi, H. Shiojiri, T. Shiotani, *Structural Faults and Repair-2006*, June 13-15, Edinburgh, (2006), Paper OCON-KOBAY (in CD-ROM).
- (17) D. G. Aggelis, T. Shiotani, *Structural Faults and Repair-2006*, June 13-15, Edinburgh, (2006), Paper OCON-SHIOT-B (in CD-ROM).
- (18) R. M. Christensen, *Journal of the Mechanics and Physics of Solids*, 38 (3) (1990), pp.379-404.
- (19) B. Budiansky, *Journal of the Mechanics and Physics of Solids*, 13 (4) (1965), pp.223-227.
- (20) R. S. Crouch, J. G. M. Wood, *Engineering Fracture Mechanics*, 35 (1/2/3) (1990), pp. 211-218.
- (21) S. Popovics, J. S. Popovics, *Cement Concrete Aggr*, 20 (2) (1998), pp.262-268.
- (22) D. G. Aggelis, D. Polyzos, T. P. Philippidis, *Journal of the Mechanics and Physics of Solids*, 53 (2005), pp.857-883.
- (23) D.G. Aggelis, T.P. Philippidis, *NDT&E International*, 37 (2004), pp.617-631.
- (24) Chaix, J. F., Garnier, V., Corneloup, G., *Ultrasonics*, 44 (2006), pp.200-210.
- (25) D. G. Aggelis, T. Shiotani, *ACI Materials J.* (2007), accepted.
- (26) T. P. Philippidis, D. G. Aggelis, *Ultrasonics*, 43 (2005), pp.584-595.
- (27) S. Popovics, J. L. Rose, J. S. Popovics, *Cement and Concrete Research*, 20 (1990), pp.259-270.
- (28) J. O. Owino, L. J. Jacobs, *Journal of Engineering Mechanics*, 125 (6) (1999), pp.637-647.
- (29) D. G. Aggelis, T. Shiotani, *Journal of the Acoustical Society of America*, 122(5), 2007 EL, pp.151-157.
- (30) D. G. Aggelis, S. V. Tsinopoulos, D., Polyzos, *Journal of the Acoustical Society of America* 116 (6) (2004), pp.3443-3452.
- (31) V. K. Kinra, C. Rousseau, *J. Wave Mater. Interaction* 2 (1987), pp.141-152.